

## Article

# Impact of Engineering Surface Treatment on Surface Properties of Biomedical TC4 Alloys under a Simulated Human Environment

Hongyun Deng<sup>1</sup>, Kuixue Xu<sup>1</sup>, Shuguang Liu<sup>1,2,\*</sup> , Chaofeng Zhang<sup>1</sup>, Xiongwei Zhu<sup>1</sup>, Haoran Zhou<sup>1</sup>, Chaoqun Xia<sup>3</sup> and Chunbao Shi<sup>1</sup>

<sup>1</sup> Beijing Chunlizhengda Medical Instruments Co., Ltd., Beijing 101100, China; denghongyun@clzd.com (H.D.); xukuixue@clzd.com (K.X.); zhangchaofeng@clzd.com (C.Z.); zhuxiongwei@clzd.com (X.Z.); zhouhaoran@clzd.com (H.Z.); shichunbao@clzd.com (C.S.)

<sup>2</sup> School of Materials Science and Engineering, University of Science and Technology Beijing, Beijing 100083, China

<sup>3</sup> School of Materials Science and Engineering, Research Institute for Energy Equipment Materials, Hebei University of Technology, Tianjin 300130, China; chaoqunxia@hebut.edu.cn

\* Correspondence: lsg\_lsglsg@hotmail.com

**Abstract:** The impact of sandblasting, anodic oxidation, and anodic oxidation after sandblasting on the surface structure and properties of titanium alloys was investigated. It was found that the surface treatments had a significant influence on the surface roughness values, contact angle values, Vickers hardness, wear resistance, and corrosion resistance of titanium alloys. The surface roughness of titanium alloys with sandblasting treatment was increased by 67% compared to untreated specimen. The Vickers hardness of titanium alloys treated with anodic oxidation after sandblasting was found to increase from 380.8 HV to 408.5 HV, which was increased by 7.3%. The surface treatments in this work improved the wear resistance of the titanium alloys to some extent, and it can be found that the wear scar width is reduced by up to 18.6%. The corrosion resistance of the titanium alloys was found to improve on anodic oxidation. Sandblasting was found to increase surface roughness and promote the formation of a porous layer during the anodization process, resulting in a slight decrease in corrosion resistance. The corrosion current density was increased by 21% compared to the untreated specimen. The corrosion current density of the titanium alloy treated with anodic oxidation decreased to  $7.01 \times 10^{-8}$  A/cm<sup>2</sup>. The corrosion current density was decreased by 24% compared to the untreated specimen. The corrosion current density of the titanium alloys treated with anodic oxidation after sandblasting decreased to  $7.63 \times 10^{-8}$  A/cm<sup>2</sup>. The corrosion current density was decreased by 8.8% compared to the specimen with anodic oxidation. The anodic oxidation provided a hydrophilic property for the surface of Ti alloys, which could show a better osseointegration characteristic than that of sandblasting. The impact of the surface treatments on surface structure and properties of titanium alloys was studied.

**Keywords:** Ti alloys; anodic oxidation; wear; corrosion resistance; surface properties



**Citation:** Deng, H.; Xu, K.; Liu, S.; Zhang, C.; Zhu, X.; Zhou, H.; Xia, C.; Shi, C. Impact of Engineering Surface Treatment on Surface Properties of Biomedical TC4 Alloys under a Simulated Human Environment. *Coatings* **2022**, *12*, 157. <https://doi.org/10.3390/coatings12020157>

Academic Editor: Maria Vittoria Diamanti

Received: 13 December 2021

Accepted: 20 January 2022

Published: 27 January 2022

**Publisher's Note:** MDPI stays neutral with regard to jurisdictional claims in published maps and institutional affiliations.



**Copyright:** © 2022 by the authors. Licensee MDPI, Basel, Switzerland. This article is an open access article distributed under the terms and conditions of the Creative Commons Attribution (CC BY) license (<https://creativecommons.org/licenses/by/4.0/>).

## 1. Introduction

Nowadays, titanium (Ti) and Ti alloys are applied in many key areas, such as ocean and aerospace engineering and the medical industry, due to their excellent combination of mechanical properties, strong corrosion resistance, and low density [1–4]. As a medical material, specifically, the TC4 alloy exhibits good processability and mechanical properties; therefore, it is applied widely in artificial joints, oral applications, and as a skull modification Ti mesh [5–7]. The formation of oxide films of Ti alloys can hinder the contact of the medium and the substrates of Ti alloys, which improve the corrosion resistance of Ti alloys [8,9]. However, Ti alloys oxide films naturally generated are relatively thin, and do

not make a significant contribution towards corrosion resistance of Ti alloys. Moreover, as a biomedical metal implant material, after Ti alloys are implanted in the human body, they may undergo corrosion due to body fluids within the human environment, and suffer abrasion from human bone or other implants. The occurrence of wear can reduce the mechanical properties of the metal material, and cause the failure of the implant [10–13], eventually leading to increased patient suffering. It has been reported that the wear debris generated due to poor wear resistance of Ti alloys can lead to osteolysis [14,15]. Therefore, improving the surface properties of medical implants using Ti alloys is urgent.

Surface modification technologies are very important methods to improve the surface properties of lightweight alloys [16–18]. Various surface modification technologies, including magnetron sputtering, sandblasting, electroless plating, anodizing, and laser surface treatment, have been applied to improve the surface properties of Ti alloys [19–23]. In actual production and processing, sandblasting and anodic oxidation are mature technologies for surface modification of Ti alloys. However, in the case of artificial joint prostheses, there are very few studies on the performance of Ti alloys after sandblasting and anodizing.

In this study, different surface treatments were carried out on the surface of the Ti alloys, including sandblasting, anodizing, and anodizing after sandblasting. The microstructures, surface roughness values, Vickers hardness, wear resistance, corrosion resistance, and contact angle value of Ti alloys were investigated. The influence of surface treatments on the microstructures and properties of the Ti alloys was carefully studied, and the related mechanism was also discussed.

## 2. Materials and Methods

### 2.1. Materials

The biomedical Ti alloys used in the present work is Ti-6Al-4V which has lower content interstitial elements C, N, and O and impurity element, Fe (material designation is TC4 ELI), compared to that of the common TC4 alloy. The elements content of Al, V, C, N, O, Fe, and H are 6%, 4%, 0.03%, 0.01%, 0.1%, 0.1%, and 0.003%, respectively. The balance is Ti. Specimens of 3 mm thickness and 14 mm diameter were cut from a bar. Then, the surfaces of the specimens were treated by finish turning (specimen A). The specimens were fine turned and washed ultrasonically in acetone and ethanol [24,25]. Finally, the surfaces of the Ti alloys were treated by different surface treatments, i.e., sandblasting (specimen B), anodic oxidation (specimen C), and anodic oxidation after sandblasting (specimen D).

### 2.2. Experimental Procedure

#### 2.2.1. Sandblasting

The specimens were placed on the sample table. A sandblasting machine (Jichuan Machinery Technology Co., Ltd., Shanghai, China) was used to treat the surface of the Ti alloys. Emery with 16 mesh was used for the sandblasting. The distance between the spray gun and specimen was 50 mm, and the treatment lasted 10–30 s. After the surfaces of the Ti alloys were treated, the specimens were cleaned and dried carefully.

#### 2.2.2. Anodic Oxidation

Before anodic oxidation, the specimens were pre-treated for 1–25 min. The specimens were anodized using an anodizing equipment for 20 min. A voltage of 30 V was applied to the specimens. The electrolyte for anodic oxidation consisted of NaOH (7.5 M/L),  $\text{Na}_2\text{C}_4\text{H}_4\text{O}_6$  (0.05 M/L),  $\text{Na}_2\text{SiO}_3$  (0.33 M/L), and EDTA (0.07 M/L); it was heated to 25 °C and was agitated during anodizing. After the surfaces of the Ti alloys were treated, the specimens were cleaned and dried carefully.

#### 2.2.3. Anodic Oxidation after Sandblasting

In the first part of the process, the specimens were treated by sandblasting. The conditions of sandblasting treatment were identical to those listed in Section 2.2.1. In the

second part of the process, the sandblasted specimens were anodized, according to the steps mentioned in Section 2.2.2.

#### 2.2.4. Analysis Methods

The surface morphology of the specimens was observed by scanning electron microscopy (SEM, JSM-7100, JEOL, Ltd., Tokyo, Japan) and atomic force microscopy (AFM, Agilent 5500, Agilent Technologies Co., Ltd., Santa Clara, CA, USA). The phase compositions of untreated and surface-treated specimens were confirmed by conventional X-ray diffraction (XRD) and Cu K $\alpha$  radiation (D/max-2500/PC), and the diffraction angle range was 20–100 degrees (step size 0.02 degrees). The microhardness of the specimens before and after surface treatment was tested by the microhardness tester (HMV-2T, Shimadzu Corp., Tokyo, Japan) with a load of 200 gf and a testing duration of 15 s. The penetration depth of the indentation tip was about 1  $\mu$ m. The wear resistance was evaluated by a Bruker UMT-5 friction and wear tester (Beijing Asia Science&Tech technology Co., Ltd., Beijing, China) with a load of 2N and a testing time of 1600s at 25 °C. Grinding ball was a Cr15 ball with 6 mm. The surface roughness values were measured by a roughometer (SRA-2, Shangguang Instruments Co., Ltd., Beijing, China) with a testing range of 1–3  $\mu$ m and testing speed of 0.5 mm/s. The CHI660E electrochemical workstation (Shanghai Chenhua Instrument Co., Ltd., Shanghai, China) and the three-electrode electrochemical cell system were used for electrochemical studies in a simulated body fluid (SBF) solution at 37 °C. The electrochemical impedance spectroscopy (EIS) of specimens were tested after the specimens were soaked for 30 min. A Pt foil electrode and saturated calomel electrode (SCE) were used as counter electrode and reference electrode, respectively. The contact angles of water on the surface of specimens were tested using a contact angle measuring instrument (DCAT21, DataPhysics Instruments, Filderstadt, Germany) equipped with a digital camera (DataPhysics Instruments, Filderstadt, Germany) at 20 °C.

### 3. Results

This section may be divided by subheadings. It should provide a concise and precise description of the experimental results, their interpretation, as well as the experimental conclusions that can be drawn.

#### 3.1. Morphologies and Structures

Figure 1 shows the macroscopic morphology of each specimen. This shows that sandblasting could significantly increase the surface roughness of the Ti alloys. In addition, black films appeared on the Ti alloys after anodizing.

Figure 2 shows the surface morphologies of the Ti alloys with different surface treatments by SEM. Grain boundaries were found on the surface of specimen A (Figure 2a). However, the grain boundaries disappeared when the Ti alloys were anodized. Moreover, some cracks and islands were found on the surface of the specimen C (Figure 2c). In addition, surface deformation was generated and grain boundaries disappeared on sandblasted for specimen B. Furthermore, some boundaries were generated on the surface of specimen B (Figure 2b). More islands were found on specimen D. However, the boundaries resulting from the sandblasting treatment were significantly reduced (Figure 2d). In addition, EDS showed O and Ti on the surface of specimens C and D (Figure 2e,f). This indicates that oxidation films of Ti alloys were formed, which is consistent with optical microscopy images (Figure 1c,d).

Figure 3 shows the AFM morphology of Ti alloys with different surface treatments. The surface of specimen A was found to be smooth (Figure 3a) and treated surfaces were rougher. Moreover, a larger number of small bumps were found on the specimen D (Figure 3d).

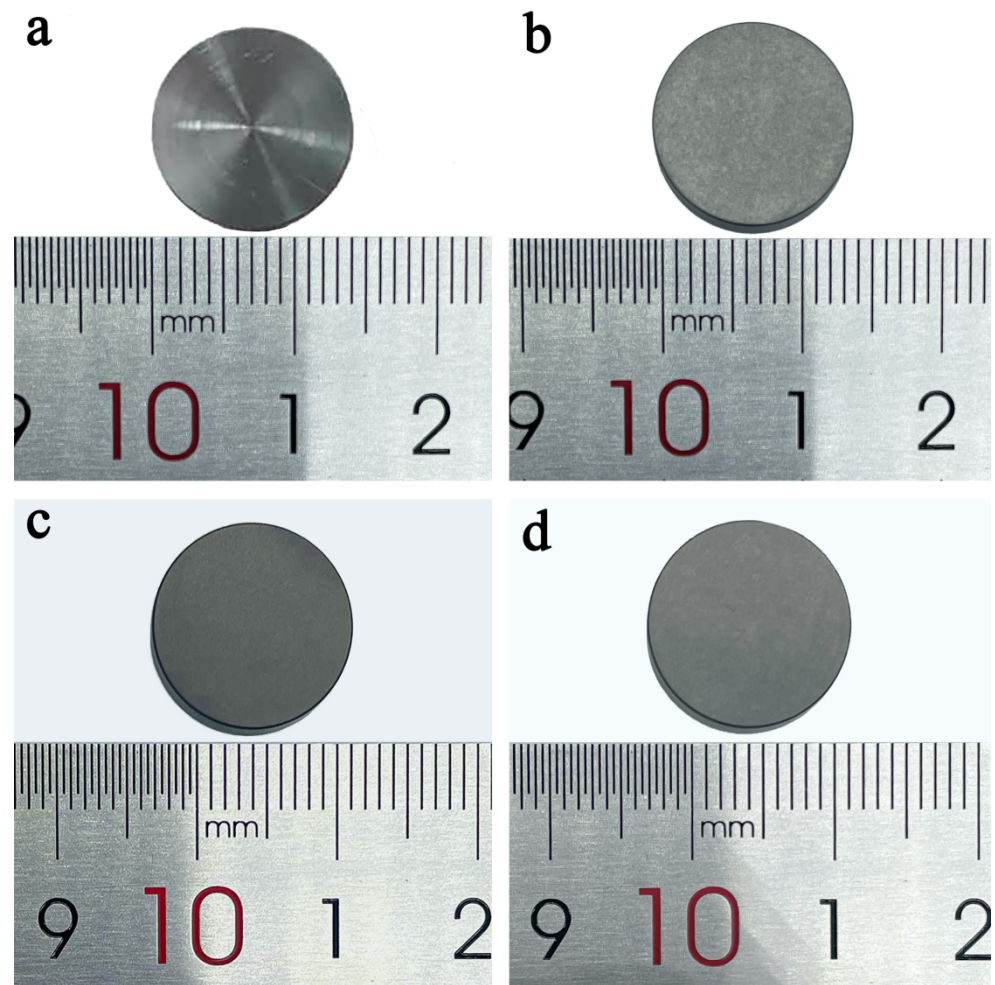


**Figure 1.** The appearance of Ti alloys with different surface treatments. (a) specimen A, (b) specimen B, (c) specimen C, and (d) specimen D.

Figure 4 shows the XRD results of the Ti alloys with different surface treatments. Three diffraction peaks with higher diffraction intensity were all substrates of Ti alloys. Moreover, the peak of titanium oxide was not found on the specimens C and D. However, the minute changes of XRD patterns can still be observed through the partial enlarged view with  $2\theta$  from 35 to 42 degrees. The XRD peak of the sample after processing of sandblasting shifted slightly towards a high angle orientation compared to the untreated sample. According to Bragg's Law ( $2d\sin\theta = n\lambda$ ), the micro residual stress produced by severe deformation within a certain depth of the surface in the process of sandblasting changed lattice parameter. The crystal plane spacing perpendicular to the surface direction is decreased. After the following anodic oxidation treatment, the stress was released by the synergistic effect of the electrolyte corrosion and oxide film growth. Therefore, the XRD peaks of sample C and D returned to normal position again. Moreover, for specimen C, it could be seen that the  $\alpha(101)$  peak shifted to the higher angles indicating a compressive strain out-of-plane[1,2] compared to specimen D. In addition, the width of the diffraction peaks slightly broadened apart from the untreated sample, which indicate that the grains were refined in the condition of identical composition after surface deformation strengthening and anodic oxidation treatment.

Figure 5 shows surface roughness values of Ti alloys with different surface treatments. It could be found that the surface roughness values of specimen C had a little change compared to that of specimen A. In addition, the surface roughness values of specimen B

were increased by 67% obviously compared to that of specimen A. Moreover, the surface roughness values of specimen D were increased by 100% compared to that of specimen A.

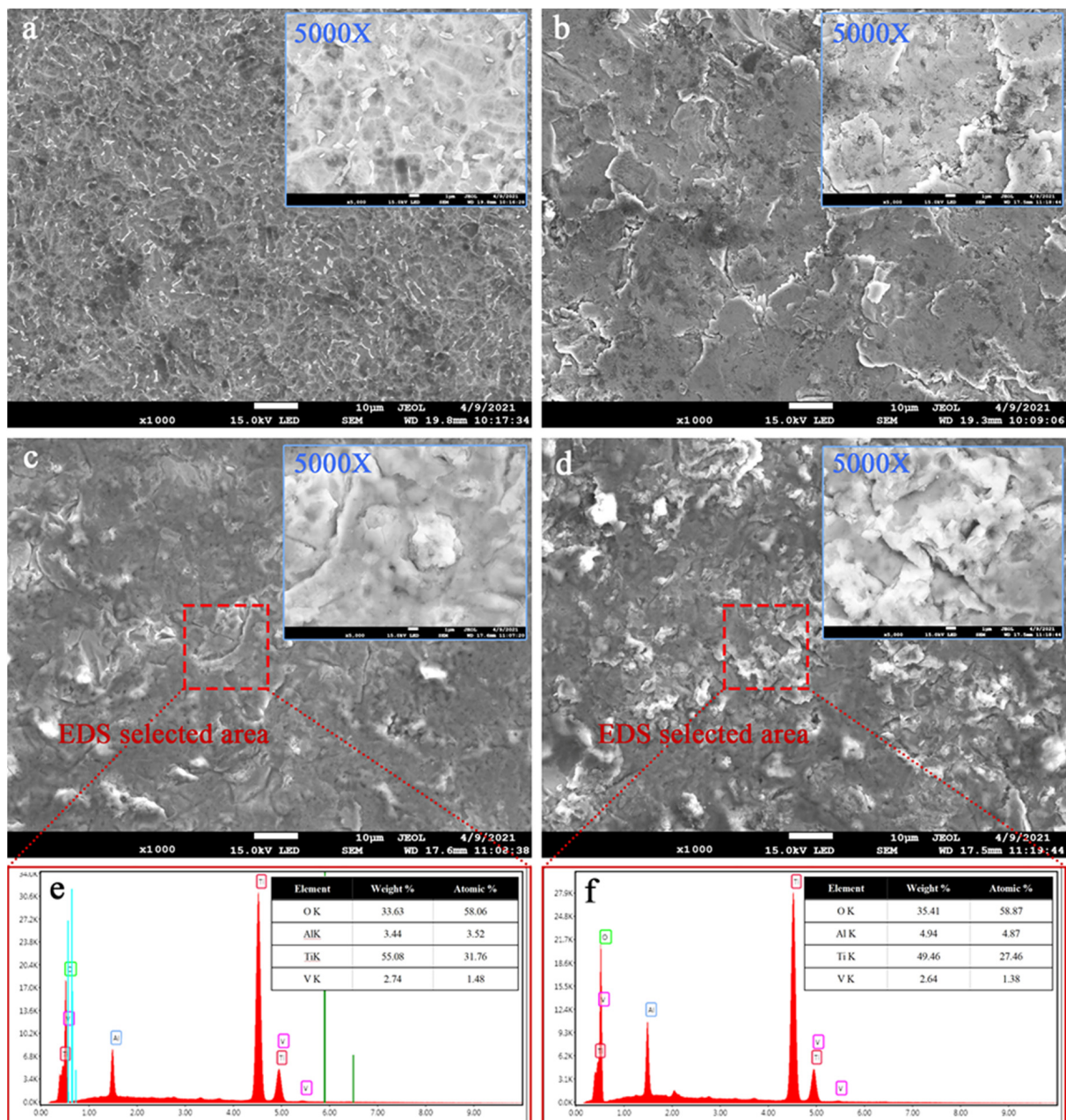


**Figure 2.** Surface morphologies of Ti alloys with different surface treatments. (a) specimen A, (b) specimen B, (c) specimen C, and (d) specimen D, (e) the EDS results of specimen C, (f) the EDS results of specimen D.

### 3.2. Mechanical Properties

Figure 6 shows the Vickers hardness of Ti alloys with different surface treatments. It could be found that the Vickers hardness of specimen C was increased to 393.4 HV, which was increased by 2.5% compared to specimen A. Moreover, the Vickers hardness of specimen B was increased to 390.7 HV, which was increased by 3.3% compared to specimen A. It also could be found that the Vickers hardness of specimen D was increased to 408.5 HV, which was increased by 7.3% compared to specimen A. Therefore, the increase in Vickers hardness of Ti alloys with various surface treatments was not significant in this work.

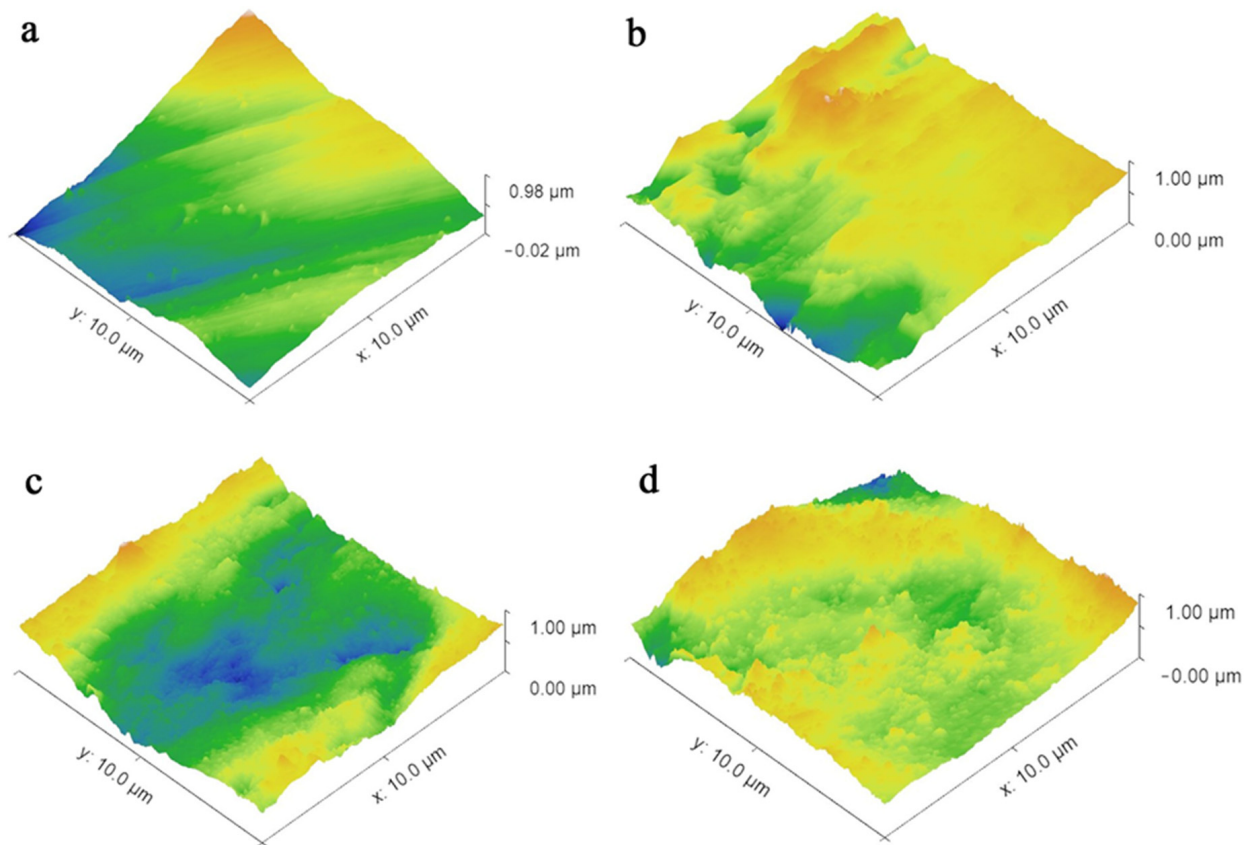


**Figure 3.** Atomic force microscopy morphology of Ti alloys with different surface treatments. (a) specimen A, (b) specimen B, (c) specimen C, and (d) specimen D.

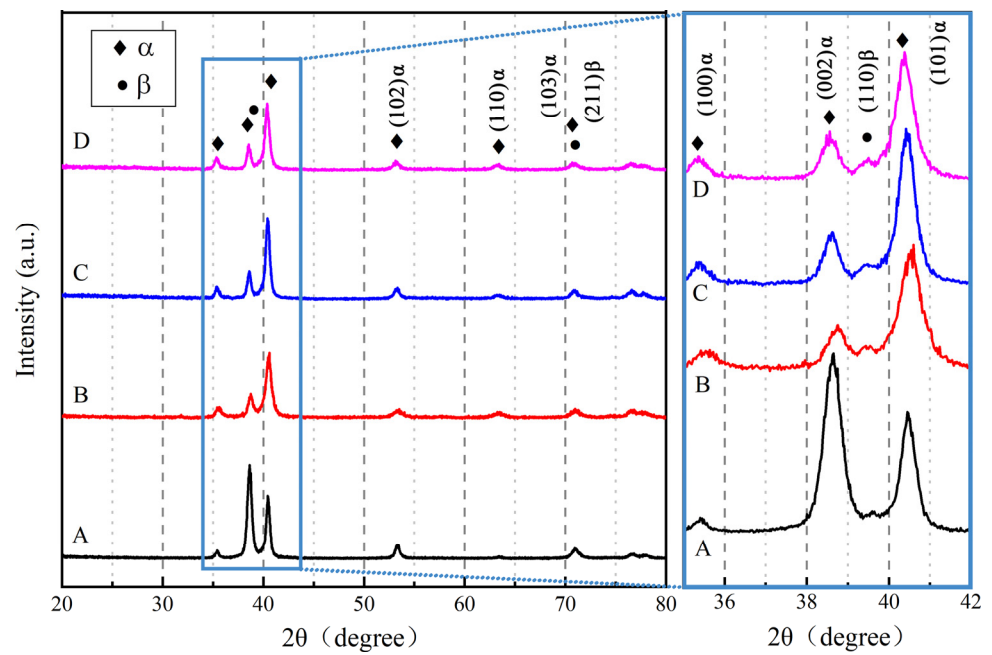


**Figure 4.** The XRD results of Ti alloys with different surface treatments. (A) specimen A, (B) specimen B, (C) specimen C, and (D) specimen D.

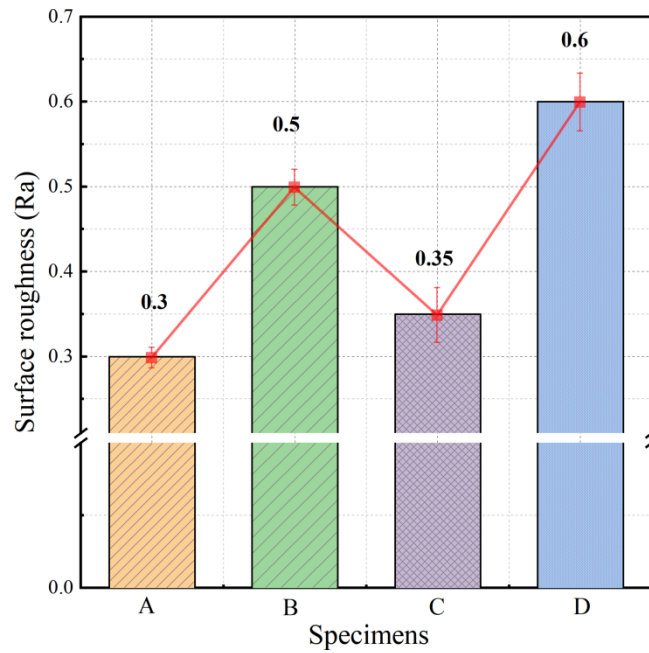


Figure 5. Surface roughness values of Ti alloys with different surface treatments.

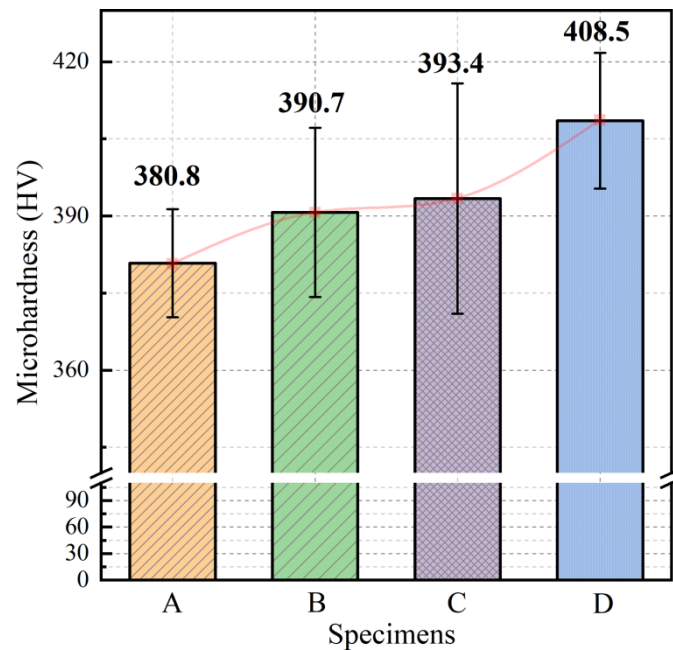
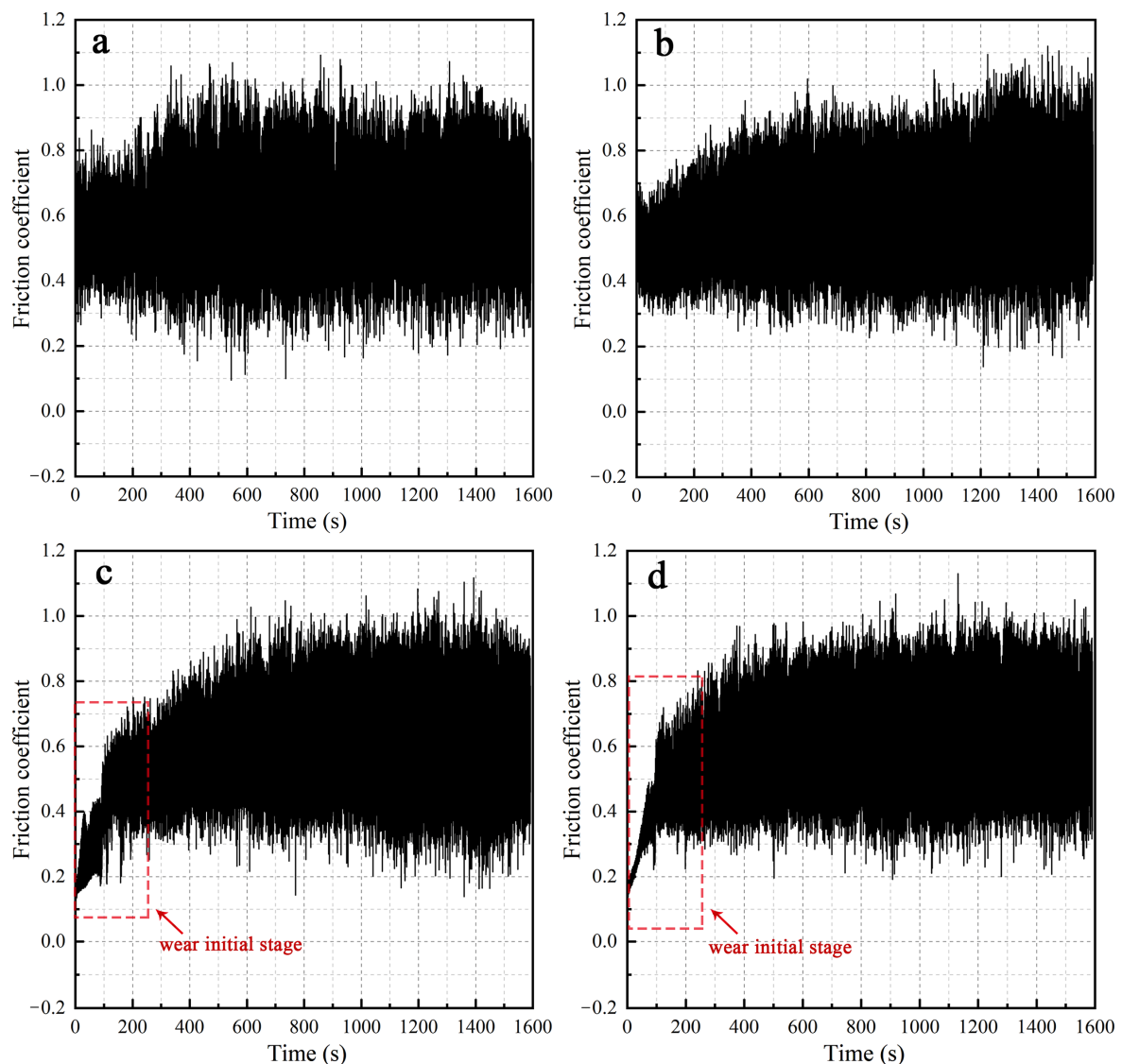


Figure 6. The Vickers hardness of Ti alloys with different surface treatments.

Figure 7 shows the variations of friction coefficients of Ti alloys with wear time. Figure 8 shows the wear morphologies of Ti alloys with different surface treatments. It could be found that friction coefficients of Ti alloys with different surface treatments had a little change in the stable stage of wear. However, it also could be found that the friction coefficients of specimens C and D were increased gradually from very low values in the initial stage of wear (Figure 7). Moreover, there are some differences in the optical images of wear morphology of Ti alloys with different surface treatments (Figure 8). The wear scar width of 980.2  $\mu\text{m}$  was found on the surface of Ti alloys without surface treatment. However, the wear marks of specimens B, C, and D were narrower, reaching wear scar width of 823.1  $\mu\text{m}$ , 798.3  $\mu\text{m}$ , and 818.2  $\mu\text{m}$ , which was decreased by 16%, 18.6%, and 16.5% compared to specimen A.



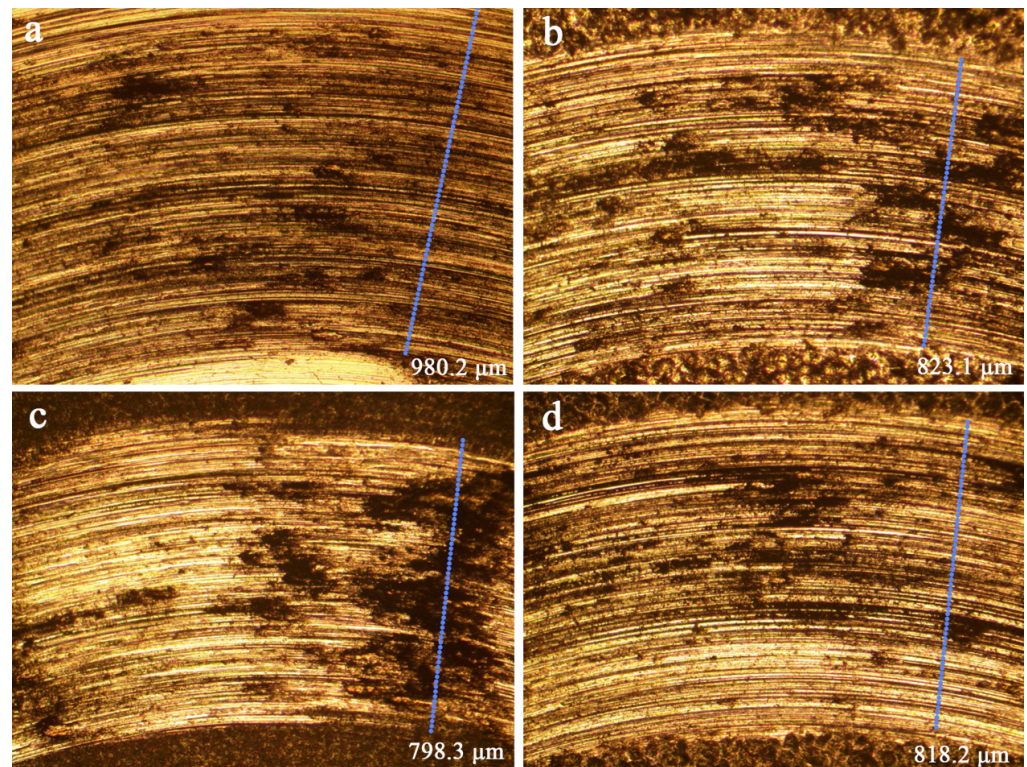
**Figure 7.** Variations of friction coefficients of Ti alloys with wear time. (a) specimen A, (b) specimen B, (c) specimen C, and (d) specimen D.

### 3.3. Corrosion Resistance

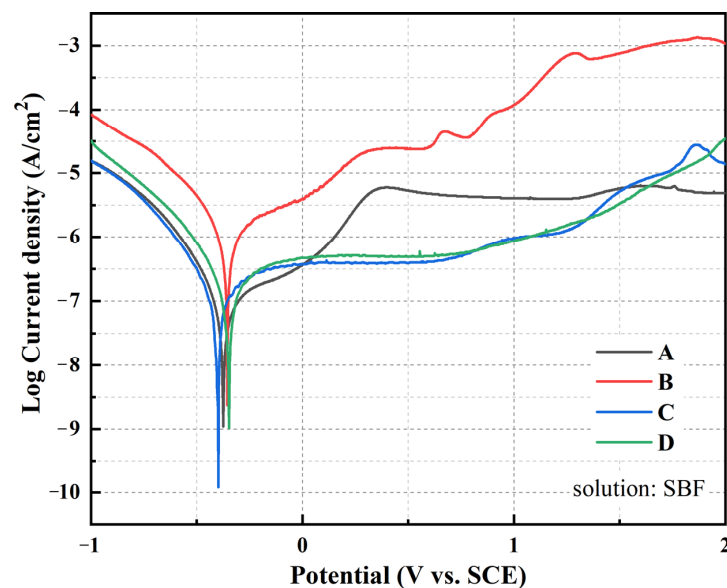
Figure 9 shows the potentiodynamic polarization curves of Ti alloys with different surface treatments in the SBF solution. The corrosion current density of specimen A was  $9.17 \times 10^{-8} \text{ A/cm}^2$ . The corrosion current density of specimen C was decreased to  $7.01 \times 10^{-8} \text{ A/cm}^2$ . The corrosion current density of specimen C was decreased by 24% compared to the specimen A. This was indicated that the corrosion resistance of Ti alloys was improved by anodic oxidation. However, the corrosion current density of specimen B was increased to  $1.11 \times 10^{-7} \text{ A/cm}^2$ . The corrosion current density of specimen B was increased by 21% compared to the specimen A. The corrosion current density of specimen D was decreased to  $7.63 \times 10^{-7} \text{ A/cm}^2$ . It was also found that corrosion current density of specimen D was increased to 8.8% compared to it of specimen C. Therefore, there was no significant difference in the corrosion current density between the specimens treated by anodic oxidation and those treated by anodic oxidation after sandblasting.

Figure 10 shows the EIS of Ti alloys with different surface treatments. It can be found that the phase angles of specimens C and D were close to  $-90$  degrees in the high frequency region. However, the phase angles of specimens A and B were close to  $-90$  degrees in the low frequency region (Figure 10a). This was indicated that the treatment of anodic

oxidation on Ti alloys changed the corrosion process of Ti alloys. Moreover, the peak width of specimen A was wider than that of specimen B. It was indicated that the corrosion resistance of specimen A was better than that of specimen B. In addition, the values of impedance modulus of specimens C and D were larger than that of specimens A and B (Figure 10b). This was indicated that the treatment of anodic oxidation improved the corrosion resistance of Ti alloys. The corrosion resistance of specimen C was found to be better than that of specimen D. This was consistent with the results of the potentiodynamic polarization curves.



**Figure 8.** Optical images of wear morphologies of Ti alloys with different surface treatments. (a) specimen A, (b) specimen B, (c) specimen C, and (d) specimen D.



**Figure 9.** The potentiodynamic polarization curves of Ti alloys with different surface treatments.

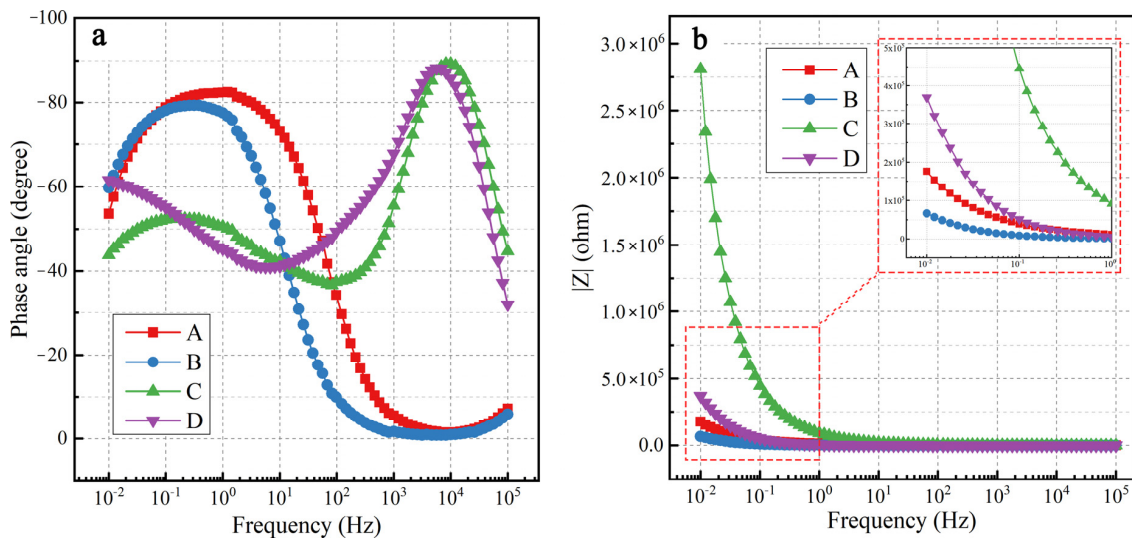


**Figure 10.** EIS of Ti alloys with different surface treatments. (a) the phase angle diagram of different specimens, (b) impedance modulus of different specimens.

3.4. Contact Angles

Figure 11 shows the contact angles of water on the surface of Ti alloys with different surface treatments. The contact angles of Ti alloys had a significant change. The contact angles of specimen A were 56.3 degrees. It was found that the contact angles of specimen C increased to 88.2 degrees. Moreover, the contact angles of specimen B were increased to 101.5 degrees. However, the contact angle value of specimen D decreased to 77.2 degrees compared to that of specimen B.

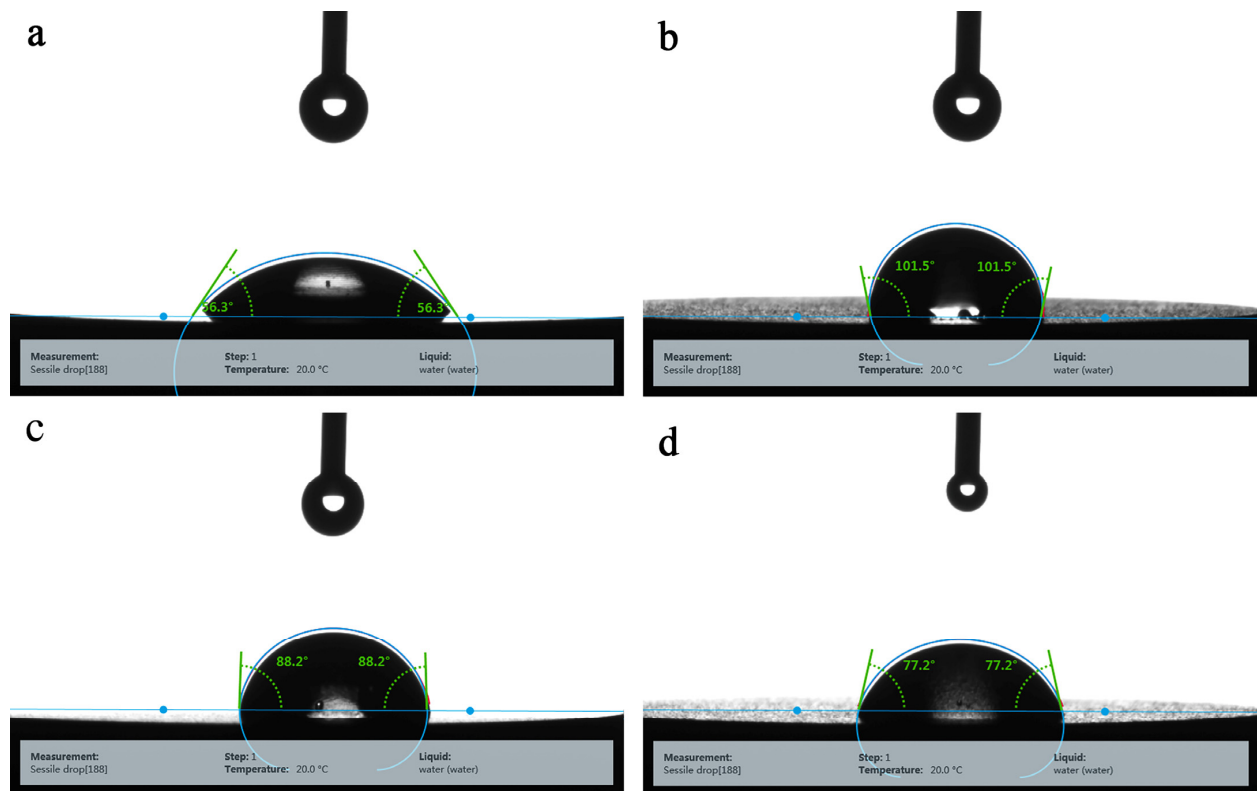


**Figure 11.** The contact angles of Ti alloys with different surface treatments. (a) specimen A, (b) specimen B, (c) specimen C, and (d) specimen D.

#### 4. Discussion

The results of morphologies of Ti alloys (Figures 1 and 2) showed that oxidation films were formed on the Ti alloys. However, the peaks of titanium oxide were not found for specimens C and D (Figure 4). The diffraction peaks are shown in Figure 4, and specimens only showed peaks for  $\alpha$  or  $\beta$  phases, with no other intermetallic phases. In other words, only nanoscale depth from the surface was affected by the anodic oxidation treatment; the phase compositions of substrate alloy and XRD detection results were unsusceptible. In addition, the analyses of results (Figures 5–10) suggest that Ti alloys with different surface treatments had different mechanical properties, wear resistance, corrosion resistance, and contact angles.

Different surface roughness values were found on the Ti alloys with different surface treatments from Figure 5. It is generally accepted that the surface roughness of Ti alloys increased on sandblasting [24]. Moreover, it can be found that the surface roughness value of Ti alloys increased with anodic oxidation after sandblasting. Thus, anodic oxidation could improve the surface roughness values, which is consistent with literature reports [25,26]. The increase of roughness can be attributed to the growth of oxidation films. Dense oxidation films were formed on the Ti alloys at the beginning of anodization. The electrolyte diffusion rate of the position in depression of the rough-surface was slow, so the generated Joule heat was more difficult to diffuse. Therefore, the dissolution rate of the layer in the concave of rough surface was increased, resulting in a decrease in membrane resistance and an increase in current and current density. This resulted in a large amount of heat, which intensified the dissolution of the films in the concave of rough surface. The Ti alloys with sandblasting were rougher; therefore, the dissolution of layers in concave of rough surface increased significantly. Moreover, the dissolution of layers would also occur where the oxidation layer was uneven. Therefore, the surface roughness value of specimen D was higher.

The surface treatments were found to improve the Vickers hardness of the Ti alloys in this study. However, the increase in the Vickers hardness resulting from surface treatment was not very significant. It is generally accepted that a certain degree of plastic deformation occurs on the surface of metal due to sandblasting, causing the lattice distortion to become larger [27]. The surface of Ti alloys was strengthened to a certain extent. Therefore, the sandblasting improved the surface hardness of the Ti alloys. Moreover, it was generally also accepted that the oxidation films of Ti alloys have a higher hardness [28]. However, surface treatments of sandblasting and anodic oxidation in this study did not significantly improve the hardness of the Ti alloys. This may be because the strengthened layer or the oxidation films prepared were thin, and were easily destroyed in the Vickers hardness test. Therefore, the Vickers hardness measured was the composite hardness of the strengthened layer/oxidation films and the substrate, resulting in an inconspicuous increase in the Vickers hardness of Ti alloys.

The friction coefficients of Ti alloys with different surface treatments had a little change in the stable stage of wear. Moreover, obvious wear marks were found on the Ti alloys with different surface treatments. It was indicated that the different surface treatments had no effective protection on Ti alloys substrate in this work. For specimens A and B, Ti alloy and grinding ball were contacted directly in wear test. There was adhesion between metals during wearing, so the friction coefficient of specimens A and B was larger. It could be found the initial friction coefficients were about 0.2 for specimens C and D. The oxidation films were generated for specimens C and D during anodizing, which hindered to Ti alloy contact with grinding ball, thereby reducing adhesion between the specimens and grinding ball in wear. Therefore, the initial friction coefficients were smaller for specimens C and D. The oxidation films were broken as the extension of wear time. The formation of wear debris increased the friction coefficients. Therefore, the friction coefficients increased gradually with the extension of wear time. The friction coefficients of specimens C and D were approached to that of specimens A and B in the stable stage of wear, indicating that substrates of specimens C and D were contacted by a grinding ball in the stable stage of

wear. In addition, narrower wear marks were found on the surface of Ti alloys with surface treatment. This indicates that the surface treatment could reduce the wear rate of the Ti alloys. It is generally also accepted that the wear resistance of materials is influenced by the hardness. The hardness of Ti alloys with surface treatments had a slight increase compared to that of Ti alloys without surface treatment. The resistance to deformation of specimens C and D was stronger during wear. Therefore, the surface treatment improved the wear resistance of Ti alloys to some extent.

The corrosion current density of specimen C was decreased by 24% compared to the specimen A, indicating improved corrosion resistance. This can be attributed to the anodic oxidation layer on the Ti, which prevents the SBF solution from contacting the Ti alloy substrates. The corrosion current density of specimen B was increased by 21% compared to the specimen A, suggesting decreased corrosion resistance. It is generally observed that sandblasting can improve the roughness value of specimens. Therefore, the corrosion area of Ti alloys increased after sandblasting, resulting in increased corrosion current density. The corrosion current density of specimen D was  $7.63 \times 10^{-8} \text{ A/cm}^2$ , which was increased by 8.8% compared to the specimen C. This can be attributed to a further increase in the surface roughness of the Ti alloy, leading to an increase in the corrosion area of the specimens. Therefore, corrosion current density of specimen D was increased slightly. Moreover, it was reported that the corrosion resistance of the Ti alloys was influenced by the formation of a barrier layer and porous layer [9].

To further analyze the corrosion behavior of the Ti alloys with different surface treatments, the equivalent circuits of specimens were established. Figure 12 shows the equivalent circuits which are used for modelling the EIS results, and the extracted parameters according to the model are presented in Table 1.

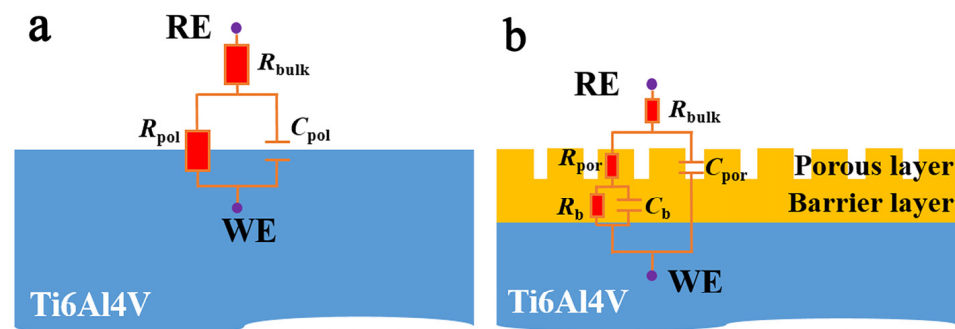


**Figure 12.** The equivalent circuits which are used for modelling the EIS results. (a) the equivalent circuit of specimens A and B; (b) the equivalent circuit of specimens C and D.

**Table 1.** Extracted parameters of different specimens according to the equivalent circuits.

Specimens	$R_{\text{bulk}} (\Omega \cdot \text{cm}^2)$	$R_{\text{pol}} (\Omega \cdot \text{cm}^2)$	$C_d (\text{F} \cdot \text{cm}^{-2})$	$R_{\text{por}} (\Omega \cdot \text{cm}^2)$	$C_{\text{por}} (\text{F} \cdot \text{cm}^{-2})$	$R_b (\Omega \cdot \text{cm}^2)$	$C_b (\text{F} \cdot \text{cm}^{-2})$
A	119	$7.4 \times 10^5$	$3 \times 10^{-5}$	-	-	-	-
B	104	$1.8 \times 10^3$	$1.6 \times 10^{-4}$	-	-	-	-
C	110	-	-	$4.5 \times 10^3$	$1.6 \times 10^{-7}$	$7.5 \times 10^6$	$2.8 \times 10^{-6}$
D	105	-	-	$2.4 \times 10^3$	$1.6 \times 10^{-6}$	$9.7 \times 10^5$	$3.2 \times 10^{-5}$

The equivalent circuit used to simulate the electrode process of specimens A and B is shown in Figure 12a, where  $C_d$  is the double-layer capacitance of the substrate,  $R_{\text{pol}}$  is the polarization resistance of substrate, and  $R_{\text{bulk}}$  is the bulk resistance of the solution. The phase angle diagram shows that there are two peaks in specimens C and D, so there are two corrosion processes for specimens C and D. The equivalent circuit used to simulate the electrode process of specimens C and D is shown in Figure 12b, where  $C_{\text{por}}$  is the capacitance of the porous layer,  $R_{\text{por}}$  is the ohmic resistance of the porous layer,  $C_b$  is the

capacitance of the barrier layer,  $R_b$  is the ohmic resistance of the barrier layer, and  $R_{bulk}$  is the bulk resistance of the solution. Table 1 shows that  $R_{por}$  and  $R_b$  of specimen C were  $4.5 \times 10^3 \Omega \cdot \text{cm}^2$  and  $7.5 \times 10^6 \Omega \cdot \text{cm}^2$ , respectively. However,  $R_{por}$  and  $R_b$  of specimen D increased to  $2.4 \times 10^3 \Omega \cdot \text{cm}^2$  and  $9.7 \times 10^5 \Omega \cdot \text{cm}^2$ , respectively. Thus, anodic oxidation films of specimen C could provide better corrosion resistance. It is generally accepted that the formation of a porous layer can decrease the corrosion resistance of the anodic oxidation film. The formation and dissolution of the film occur simultaneously during anodic oxidation. However, significant heat is generated in the cavities on the films, which may not be released during anodization, resulting in the dissolution of films in the cavities. Therefore, the formation of the porous layer was accelerated. The surface roughness of Ti alloys without sandblasting was found to be low. Therefore, a small number of cavities were generated during anodization. After sandblasting, Ti alloys had higher roughness on the surface. This allowed the Ti alloys to have more cavities during anodization, resulting in the promotion of the formation of porous layers and the dissolution of barrier layers. This resulted in a decrease in the  $R_{por}$  and  $R_b$  of specimen D.

Through the above analysis, the anodic oxidation diagram of specimens before and after sandblasting was given (Figure 13). The surface of the specimen was relatively smooth for the unsandblasted specimen, so the porous layer formed was relatively thin and had fewer voids in anodizing. However, after sandblasting, the surface roughness increased, promoting the formation of the porous layer and an increase in thickness of the porous layer during the anodization process.

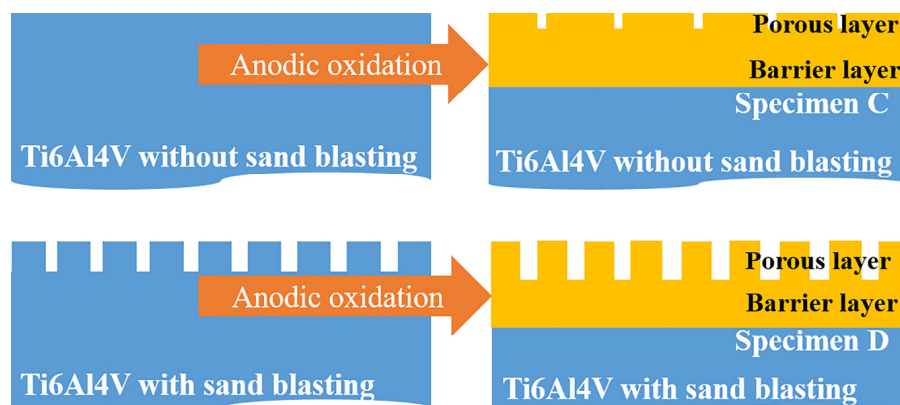


**Figure 13.** Anodic oxidation diagram of specimens before and after sandblasting.

Hydrophilicity is an important property for biomaterials [29,30]. The hydrophilic property is mainly related to the contact angles [31]. According to the relations between wetting tension and the wetting of a solid, the macroscopic result shows the high wettability (i.e., hydrophilicity) when the contact angles are between 0 and 90 degrees, and the low wettability (i.e., hydrophobicity) when the contact angles is between 90 and 180 degrees [32]. Gittens et al. [31] reported that the hydrophilic surface interacts closely with biological fluids, allowing normal protein adsorption to the surface and subsequent interactions with cell receptors. However, the hydrophobic surfaces are prone to hydrocarbon contamination, leading to entrapment of air bubbles that can interfere with protein adsorption and cell receptor adhesion/activation. In this study, the contact angle of the Ti alloy without treatments was 56.3 degrees, which showed a good hydrophilic property. After sandblasting, the contact angles of specimen B increased to 101.5 degrees showing the hydrophobicity which was not conducive to the adsorption of osteoblast cells. The contact angles of the specimens C and D, which were treated by anodic oxidation, were found to be 88.2 degrees and 77.2 degrees, respectively, revealing a similar hydrophilic level. In actual production and processing, the surface treatment of Ti-alloy implants is the sandblasting rather than stopping at the finish turning. Therefore, only the surface treatment of sandblasting and surface anodic oxidation could be applied to the implant prosthesis products. In conclusion,

the anodic oxidation provided a hydrophilic property for the surface of Ti alloys, which could show a better osseointegration characteristic than that of sandblasting.

## 5. Conclusions

The influence of the different surface treatments on the microstructure and surface properties of the Ti alloys was investigated. The following conclusions could be drawn based on the present results.

The different surface treatments improved the Vickers hardness of Ti alloys slightly. The Vickers hardness of Ti alloys treated by anodic oxidation after sandblasting was increased from 380.8 HV to 408.5 HV, which was increased by 7.3%. In addition, the surface treatments by anodic oxidation decreased wear scar widths by 18.6% compared to the untreated specimen, which improved the wear resistance of the Ti alloys.

The treatment of anodic oxidation improves the corrosion resistance of Ti alloys, which was found to be decreased by 24% in corrosion current density compared to the untreated specimen. Sandblasting increased the roughness and promoted the formation of the porous layer during the anodization process, resulting in a decrease in corrosion resistance of Ti alloys, which was increased by 8.8% in corrosion current density compared to the specimen with anodic oxidation.

The contact angle of Ti alloys after anodizing was 88.2 degrees. The contact angle of Ti alloys treated by anodic oxidation after sandblasting was 77.2 degrees. The anodic oxidation provided a hydrophilic property for the surface of Ti alloys, which could show a better osseointegration characteristic than that of sandblasting.

**Author Contributions:** Conceptualization and funding acquisition, S.L.; writing and formal analysis, H.D.; project administration, K.X.; resources, C.Z.; methodology and investigation, X.Z., H.Z.; review and editing, S.L., H.D.; data curation and validation, C.X.; supervision, C.S. All authors have read and agreed to the published version of the manuscript.

**Funding:** This work was supported by the National Key Research and Development Program of China (Grant No. 2020YFC1107502), the China Postdoctoral Science Foundation (Grant No. 2021M700490), and the Beijing Postdoctoral Research Foundation (Grant No. 2021-ZZ-075).

**Institutional Review Board Statement:** Not applicable.

**Informed Consent Statement:** Not applicable.

**Data Availability Statement:** The raw/processed data required to reproduce these findings cannot be shared at this time as the data also form part of an ongoing study.

**Acknowledgments:** Special thanks go to Pengfei Ji and Tianshuo Song for experimental assistance.

**Conflicts of Interest:** The authors declare no conflict of interest.

## References

1. Liu, S.G.; Xia, C.Q.; Feng, Z.H.; Zhang, X.; Chen, B.H.; Xie, C.L.; Zhou, Y.K.; Zhang, X.Y.; Ma, M.Z.; Liu, R.P. Influence of phase composition and microstructure on mechanical properties of hot-rolled Ti- $\chi$ Zr-4Al-0.005B alloys. *J. Alloys Compd.* **2018**, *751*, 247–256. [[CrossRef](#)]
2. Yang, J.L.; Wang, G.F.; Zhang, W.C.; Chen, W.Z.; Jiao, X.Y.; Zhang, K.F. Microstructure evolution and mechanical properties of P/M Ti-22Al-25Nb alloy during hot extrusion. *Mater. Sci. Eng. A.* **2017**, *699*, 210–216. [[CrossRef](#)]
3. Li, X.X.; Yang, C.; Lu, H.Z.; Luo, X.; Lvasishin, O.M. Correlation between atomic diffusivity and densification mechanism during spark plasma sintering of titanium alloy powders. *J. Alloys Compd.* **2019**, *787*, 112–122. [[CrossRef](#)]
4. Qiu, K.J.; Liu, Y.; Zhou, F.Y.; Wang, B.L.; Li, L.; Zheng, Y.F.; Liu, Y.H. Microstructure, mechanical properties, castability and in vitro biocompatibility of Ti-Bi alloys developed for dental applications. *Acta Biomater.* **2015**, *15*, 254–265. [[CrossRef](#)]
5. Ellis, E.; Tan, Y.H. Assessment of internal orbital reconstructions for pure blowout fractures: Cranial bone grafts versus titanium mesh. *J. Oral Maxillofac. Surg.* **2003**, *61*, 442–453. [[CrossRef](#)] [[PubMed](#)]
6. Liu, X.Y.; Chu, P.K.; Ding, C.X. Surface modification of titanium, titanium alloys, and related materials for biomedical applications. *Mater. Sci. Eng. R* **2004**, *47*, 49–121. [[CrossRef](#)]
7. Dikova, T.; Milkov, M. Application of Ti and Ti alloys in dental implantology. *Int. J. Tuberc. Lung Dis.* **2013**, *17*, 48–50.
8. Marbacher, S.; Andres, R.H.; Fathi, A.-R.; Fandino, J. Primary reconstruction of open depressed skull fractures with titanium mesh. *J. Craniofacial Surg.* **2008**, *19*, 490–495. [[CrossRef](#)]

9. Assis, S.; Wolyneć, S.; Costa, I. Corrosion characterization of titanium alloys by electrochemical techniques. *Electrochim. Acta* **2006**, *51*, 1815–1819. [[CrossRef](#)]
10. González, J.E.G.; Mirza-Rosca, J.C. Study of the corrosion behavior of titanium of its alloys for biomedical and dental implant applications. *J. Electroanal. Chem.* **1999**, *471*, 109–115. [[CrossRef](#)]
11. Sathish, S.; Geetha, M.; Pandey, N.D.; Richard, C.; Asokamani, R. Studies on the corrosion and wear behavior of the laser nitrided biomedical titanium and its alloys. *Mater. Sci. Eng. C* **2010**, *30*, 376–382. [[CrossRef](#)]
12. Vadiraj, A.; Kamaraj, M.; Gnanamoorthy, R. Fretting wear studies on uncoated, plasma nitrided and laser nitrided biomedical titanium alloys. *Mater. Sci. Eng. A* **2007**, *445*, 446–453. [[CrossRef](#)]
13. Engh Jr, C.A.; Moore, K.D.; Vinh, T.N.; Engh, G.A. Titanium prosthetic wear debris in remote bone marrow. A report of two cases. *J. Bone Jt. Surg.* **1997**, *79*, 1721–1725. [[CrossRef](#)] [[PubMed](#)]
14. Buly, R.L.; Huo, M.H.; Salvati, E.; Brien, W.; Bansal, M. Titanium wear debris in failed cemented total hip arthroplasty. An analysis of 71 cases. *J. Arthroplast.* **1992**, *7*, 315–323. [[CrossRef](#)]
15. Buchanan, R.A.; Rigney Jr, E.D.; Williams, J.M. Ion implantation of surgical Ti-6Al-4V for improved resistance to wear-accelerated corrosion. *J. Biomed. Mater. Res. Part A* **1987**, *21*, 55–366. [[CrossRef](#)] [[PubMed](#)]
16. Zhang, L.C.; Chen, L.Y.; Wang, L.Q. Surface Modification of Titanium and Titanium Alloys: Technologies, Developments, and Future Interests. *Adv. Eng. Mater.* **2019**, *22*, 1901258. [[CrossRef](#)]
17. Deng, H.Y.; Chen, D.X.; Wang, Y.N.; Zhou, Y.W.; Gao, P. Effects of silicon on microstructure and corrosion resistance of diamond-like-carbon film prepared on 2024 aluminum alloy by plasma-enhanced chemical vapor deposition. *Diam. Relat. Mater.* **2020**, *110*, 108144. [[CrossRef](#)]
18. Hiraga, H.; Inoue, T.; Kojima, Y.; Kamado, S.; Watanabe, S. Surface modification by dispersion of hard particles on magnesium alloy with laser. *Mater. Sci. Forum* **2000**, *350–351*, 253–260. [[CrossRef](#)]
19. Qi, J.W.; Yang, Y.M.; Zhou, M.M.; Chen, Z.B.; Chen, K. Effect of transition layer on the performance of hydroxyapatite/titanium nitride coating developed on Ti-6Al-4V alloy by magnetron sputtering. *Ceram. Int.* **2019**, *45*, 4863–4869. [[CrossRef](#)]
20. Li, D.H.; Liu, B.L.; Han, Y.; Xu, K.W. Effects of a Modified sandblasting surface treatment on topographic and chemical properties of titanium surface. *Implant. Dent.* **2001**, *10*, 59–64. [[CrossRef](#)]
21. Tang, E.J.; Liu, Z.; Zhao, Y.Q. A Study of electroless Ni-P plating on titanium alloy. *Electroplating. Pollut. Control* **2003**, *23*, 21–22.
22. Song, H.J.; Kim, M.K.; Jung, G.C.; Vang, M.S.; Park, Y.J. The effects of spark anodizing treatment of pure titanium metals and titanium alloys on corrosion characteristics. *Surf. Coat. Technol.* **2007**, *201*, 8738–8745. [[CrossRef](#)]
23. Tian, Y.S.; Chen, C.Z.; Li, S.T.; Huo, Q.H. Research progress on laser surface modification of titanium alloys. *Appl. Surf. Sci.* **2005**, *242*, 177–184. [[CrossRef](#)]
24. Khanlou, H.M.; Ang, B.C.; Barzani, M.M.; Silakhori, M.; Talebian, S. Prediction and characterization of surface roughness using sandblasting and acid etching process on new non-toxic titanium biomaterial: Adaptive-network-based fuzzy inference System. *Neural Comput. Appl.* **2015**, *26*, 1751–1761. [[CrossRef](#)]
25. Wu, L.; Liu, J.H.; Wu, G.L.; Li, S.M.; Yu, M. Growth behaviour of anodic oxide film on titanium alloy. *Surf. Eng.* **2015**, *33*, 841–848. [[CrossRef](#)]
26. Li, B.; Li, J.; Liang, C.; Li, H.; Liu, S.; Wang, H. Surface Roughness and hydrophilicity of titanium after anodic oxidation. *Rare Met. Mater. Eng.* **2016**, *45*, 858–862. [[CrossRef](#)]
27. Arifvianto, B.; Suyitno, S.; Mahardika, M. Effect of sandblasting and surface mechanical attrition treatment on surface roughness, wettability, and microhardness distribution of aisi 316l. *Key Eng. Mater.* **2011**, *462–463*, 738–743. [[CrossRef](#)]
28. Pang, M.; Eakins, D.E.; Norton, M.G.; Bahr, D.F. Structural and mechanical characteristics of anodic oxide films on titanium. *Corrosion* **2001**, *57*, 523–531. [[CrossRef](#)]
29. Schwarz, F.; Wieland, M.; Schwartz, Z.; Zhao, G.; Rupp, F.; Geis-Gerstorfer, J.; Schedle, A.; Broggini, N.; Bornstein, M.M.; Buser, D.; et al. Potential of chemically modified hydrophilic surface characteristics to support tissue integration of titanium dental implants. *Biomed. Mater. Res. B* **2009**, *88*, 544–557. [[CrossRef](#)]
30. Rupp, F.; Scheideler, L.; Eichler, M.; Geis-Gerstorfer, J. Wetting behavior of dental implants. *Int. J. Oral Maxillofac. Implant.* **2011**, *26*, 1256–1266.
31. Gittens, R.A.; Scheideler, L.; Rupp, F.; Hyzy, S.L.; Geis-Gerstorfer, J.; Schwartz, Z.; Boyan, B.D. A review on the wettability of dental implant surfaces II: Biological and clinical aspects. *Acta Biomater.* **2014**, *10*, 2907–2918. [[CrossRef](#)] [[PubMed](#)]
32. Rupp, F.; Gittens, R.A.; Scheideler, L.; Marmur, A.; Boyan, B.D.; Schwartz, Z.; Geis-Gerstorfer, J. A review on the wettability of dental implant surfaces I: Theoretical and experimental aspects. *Acta Biomater.* **2014**, *10*, 2894–2906. [[CrossRef](#)] [[PubMed](#)]